

---

# Asynchronous Batch Bayesian Optimisation with Improved Local Penalisation

---

Ahsan S. Alvi<sup>\*12</sup> Binxin Ru<sup>\*1</sup> Jan Calliess<sup>13</sup> Stephen J. Roberts<sup>123</sup> Michael A. Osborne<sup>12</sup>

## Abstract

Batch Bayesian optimisation (BO) has been successfully applied to hyperparameter tuning using parallel computing, but it is wasteful of resources: workers that complete jobs ahead of others are left idle. We address this problem by developing an approach, *Penalising Locally for Asynchronous Bayesian Optimisation on  $k$  workers* (PLAyBOOK), for asynchronous parallel BO. We demonstrate empirically the efficacy of PLaYBOOK and its variants on synthetic tasks and a real-world problem. We undertake a comparison between synchronous and asynchronous BO, and show that asynchronous BO often outperforms synchronous batch BO in both wall-clock time and number of function evaluations.

## 1. Introduction

Bayesian optimisation (BO) is a popular sequential global optimisation technique for functions that are expensive to evaluate (Brochu et al., 2010). Whilst standard BO may be sufficient for many applications, it is often the case that multiple experiments can be run at the same time in parallel. For example, in the case of drug discovery, many different compounds can be tested in parallel via high throughput screening equipment (Hernández-Lobato et al., 2017), and when optimising machine learning algorithms, we can train different model configurations concurrently on multiple workers (Chen et al., 2018; Kandasamy et al., 2018). This observation lead to the development of parallel (“batch”) BO algorithms, which, at each optimisation step, recommend a batch of  $k$  configurations to be evaluated.

In cases where the runtimes of tasks are roughly equal, this is usually sufficient, but, if the runtimes in a batch vary, this will lead to inefficient utilisation of our hardware. For

<sup>\*</sup>Equal contribution <sup>1</sup>Department of Engineering Science, University of Oxford <sup>2</sup>Mind Foundry Ltd., Oxford, UK <sup>3</sup>Oxford-Man Institute of Quantitative Finance. Correspondence to: Binxin Ru <robin@robots.ox.ac.uk>, Ahsan Alvi <asa@robots.ox.ac.uk>.

example, consider the optimisation of the number of units in the layers of a neural network. Training and evaluating a large network (greater number of units per layer) will take significantly longer than a small network (fewer units per layer), so for an iteration of (synchronous) batch BO to complete, we need to wait for the slowest configuration in the batch to finish, leaving the other workers idle. In order to improve the utilisation of parallel computing resources, we can run function evaluations *asynchronously*: as soon as  $c$  workers ( $c < k$ ) complete their jobs, we choose new tasks for them.

Although asynchronous batch BO has a clear advantage over synchronous batch BO in terms of wall-clock time (Kandasamy et al., 2018), it may lose out in terms of sample efficiency, as an asynchronous method takes decisions with less data than its synchronous counterpart at each stage of the optimisation. We investigate this empirically in this work.

Our contributions can be summarised as follows.

- We develop a new approach to asynchronous parallel BO, *Penalising Locally for Asynchronous Bayesian Optimisation on  $k$  workers* (PLAyBOOK), which uses penalisation-based strategies to prevent redundant batch selection. We show that our approach compares favourably against existing asynchronous methods.
- We propose a new penalisation function, which prevents redundant samples from being chosen. We also propose designing the penalisers using local (instead of global) variability features of the surrogate to more effectively explore the search space.
- We demonstrate empirically that asynchronous methods perform at least as well as their synchronous variants. We also show that PLaYBOOK outperforms its synchronous variants *both* in terms of wall-clock time and sample efficiency, particularly for larger batch sizes. This renders PLaYBOOK a competitive parallel BO method.

## 2. Related work

Many different synchronous batch BO methods have been proposed over the past years. Approaches include using

hallucinated observations (Ginsbourger et al., 2010; Desautels et al., 2014), knowledge gradient (Wu & Frazier, 2016), Determinantal point processes (Kathuria et al., 2016), maximising the information gained about the objective function or the global minimiser (Contal et al., 2013; Shah & Ghahramani, 2015), and sampling-based simulation (Azimi et al., 2010; Kandasamy et al., 2018; Hernández-Lobato et al., 2017). A recent synchronous batch BO method that demonstrated promising empirical results is Local Penalisation (LP) (González et al., 2016). After adding a configuration  $x_j$  to the batch, LP penalises the value of the acquisition function in the neighbourhood of  $x_j$ , encouraging diversity in the batch selection.

Asynchronous BO has received surprisingly little attention compared to synchronous BO to date. Ginsbourger et al. (2011) proposed a sampling-based approach that approximately marginalises out the unknown function values at busy locations by taking samples from the posterior at those locations. Due to its reliance on sampling, it suffers from poor scaling, both in batch size and BO steps.

Wang et al. (2016) developed an efficient global optimiser (MOE) which estimates the gradient of q-EI, a batch BO method proposed by Ginsbourger et al. (2008), and uses it in a stochastic gradient ascent algorithm to solve the prohibitively-expensive maximisation of the q-EI acquisition function, which selects all points in the batch simultaneously.

A more recent method utilizes Thompson Sampling (Kandasamy et al., 2018) (TS) to select new batch points. This has the benefit of attractive scaling, since the method minimises samples from the surrogate model’s posterior. In the case of a Gaussian process (GP) model, a batch point is placed at the minimum location of a draw from a multivariate Gaussian distribution. The disadvantage of TS is that it relies on the uncertainty in the surrogate model to ensure that the batch points are well-distributed in the search space.

### 3. Preliminaries

To perform Bayesian optimisation to find the global minimum of an expensive objective function  $f$ , we must first decide on a surrogate model for  $f$ . Using a Gaussian process (GP) as the surrogate model is a popular choice, due to the GP’s potent function approximation properties and ability to quantify uncertainty. A GP is a prior over functions that allows us to encode our prior beliefs about the properties of the function  $f$ , such as smoothness and periodicity. A comprehensive introduction to GPs can be found in (Rasmussen & Williams, 2006).

For a scalar-valued function  $f$  defined over a compact space  $\mathcal{X}: \mathbb{R}^d \rightarrow \mathbb{R}$ , we define a GP prior over  $f$  to be  $\mathcal{GP}(m(x), k(x, x'; \theta))$  where  $m(x)$  is the mean function,

$k(\cdot, \cdot)$  is a covariance function (also known as the kernel) and  $\theta$  are the hyperparameters of the kernel. The posterior distribution of the GP at an input  $\tilde{x}$  is Gaussian:

$$p(f(\tilde{x}) \mid \tilde{x}, \mathcal{D}_s) = \mathcal{N}(f(\tilde{x}); \mu(\tilde{x}), \sigma^2(\tilde{x})), \quad (1)$$

with mean and variance

$$\mu(\tilde{x}) = k(\tilde{x}, X)K(X, X)^{-1}Y, \quad (2)$$

$$\sigma^2(\tilde{x}) = k(\tilde{x}, \tilde{x}') - k(\tilde{x}, X)K(X, X)^{-1}k(X, \tilde{x}'), \quad (3)$$

where  $X$  is a matrix with an input location in each row  $\{x_1, x_2, \dots, x_N\}$  and  $Y$  is a column vector of the corresponding observations  $\{y_1, y_2, \dots, y_N\}$ , where  $y_i = f(x_i)$ . The hyperparameters of the model have been dropped in these equations for clarity.

The second choice we make is that of the acquisition function  $\alpha: \mathbb{R}^d \rightarrow \mathbb{R}$ . Many different functional forms for  $\alpha(x)$  have been proposed to date (Kushner, 1964; Jones et al., 1998; Srinivas et al., 2010; Hennig & Schuler, 2012; Hernández-Lobato et al., 2014; Ru et al., 2018), each with their relative merits and disadvantages. Although our method is applicable to most acquisition functions, we use the popular GP Upper Confidence Bound (UCB) in our experiments (Srinivas et al., 2010). UCB is defined as

$$\alpha_{\text{UCB}}(x) = \mu(x) + \kappa\sigma(x), \quad (4)$$

where  $\mu(x)$  and  $\sigma(x)$  are the mean and standard deviation of the GP posterior and  $\kappa$  is a parameter that controls the trade-off between exploration (visiting unexplored areas in  $\mathcal{X}$ ) and exploitation (refining our belief by querying close to previous samples). This parameter can be set according to an annealing schedule (Srinivas et al., 2010) or fixed to a constant value.

### 4. Asynchronous vs synchronous BO

In synchronous BO, the aim is to select a batch of promising locations  $\mathcal{B} = \{x_j\}_{j=1}^k$  that will be evaluated in parallel (Fig. 1). Solving this task directly is difficult, which is why most batch BO algorithms convert this selection into a sequential procedure, selecting one point at a time for the batch. At the  $s$ th BO step, the optimal choice of batch point  $x_j$  ( $j \in \{1, 2, \dots, k\}$ ) should then not only take into account our current knowledge of  $f$ , but also marginalise over possible function values at the locations  $\{x_i\}_{i=1}^{j-1}$  that we have chosen so far for the batch:

$$x_j = \arg \max_{x \in \mathcal{X}} \int \alpha(x \mid \mathcal{D}_s, \mathcal{D}_{j-1}) \prod_{i=1}^{j-1} p(y_i \mid x_i, \mathcal{D}_s, \mathcal{D}_{i-1}) dy_i, \quad (5)$$

where  $\mathcal{D}_s$  are the observations we have gathered so far and  $\mathcal{D}_{j-1} = \{x_i, y_i\}_{i=1}^{j-1}$  and  $\mathcal{D}_0 = \emptyset$  (González et al., 2016).

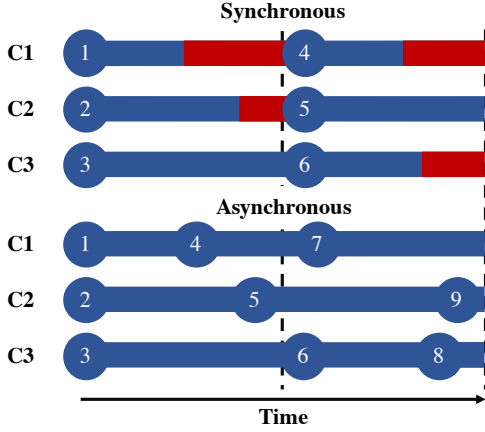


Figure 1. Illustration showing the difference between synchronous and asynchronous batch BO in the case of  $k = 3$  parallel workers. The blue bar indicates the processing time taken for a worker to evaluate its assigned task and the red bar indicates the waiting time for a worker between completing its previous task and beginning a new task. It is clear that asynchronous batch BO, which makes better use of the computing resources, can complete a greater number of evaluations than its synchronous counterpart within the same duration.

In asynchronous BO, the key motivation is to maximise the utilisation of our  $k$  parallel workers. After a desired number of workers  $c < k$  complete their tasks, we assign new tasks to them without waiting for the remaining  $b = (k - c)$  busy workers to complete their tasks. Now the general design for selecting the next query point marginalises over the likely function values both at locations under evaluation by busy workers, as well as the already-selected points in the batch:

$$x_j = \arg \max_{x \in \mathcal{X}} \iint \alpha(x \mid \mathcal{D}_{s_-}, \mathcal{D}_b, \mathcal{D}_{j-1}) \prod_{i=1}^{j-1} p(y_i \mid x_i, \mathcal{D}_{s_-}, \mathcal{D}_b, \mathcal{D}_{i-1}) \prod_{l=1}^b p(y_l \mid x_l, \mathcal{D}_{s_-}) dy_i dy_l, \quad (6)$$

where  $j \in \{1, \dots, c\}$  and  $\mathcal{D}_b = \{x_i, y_i\}_{i=1}^b$  represents the locations and function values of the busy locations.  $\mathcal{D}_{s_-}$  are the observations available at the point of constructing the asynchronous batch. In general,  $\mathcal{D}_{s_-}$  contains fewer observations than the  $\mathcal{D}_s$  that would be used to select the equivalent batch of evaluations in the synchronous setting. Fig. 1 shows the case of  $c = 1$  and thus  $b = k - 1 = 2$ .

In a given period of time, asynchronous batch BO is able to process a greater number of evaluations than the synchronous approach: asynchronous BO offers clear gains in resource utilisation. However, Kandasamy et al. (2018)

claim that the asynchronous setting may not lead to better performance when measured by the number of evaluations. The authors point out that a new evaluation in a sequentially-selected synchronous batch will be selected with at most  $k - 1$  evaluations “missing” (that is, with knowledge of their locations  $x$  but absent the knowledge of their values  $y$ ), corresponding to the previously-selected points in the current batch (i.e.  $j - 1 \leq k - 1$  in Eq. (5)). Evaluations in the asynchronous case are always chosen with  $k - 1$  “missing” evaluations.

However, to our knowledge, there exists little empirical investigation of the performance difference between synchronous and asynchronous batch methods. We conducted this comparison on a large set of benchmark test functions and found that asynchronous batch BO can be as good as synchronous batch BO for different batch selection methods. Additionally, for the penalisation-based methods we propose, asynchronous operation often outperforms the synchronous setting, particularly as the batch size increases. We will discuss this interesting empirical observation in Section 6.2.

## 5. Penalisation-based asynchronous BO

We now present our core algorithmic contributions. As discussed in Section 2, the existing asynchronous BO methods suffer drawbacks such as the prohibitively high cost of repeatedly updating GP surrogates when selecting batch points (Ginsbourger et al., 2011) or the risk of redundant sampling at or near a busy location in the batch (Kandasamy et al., 2018). In view of these limitations, we propose a penalisation-based asynchronous method which encourages sampling diversity among the points in the batch as well as eliminating the risk of repeated samples in the same batch. Our proposed method remains computationally efficient, and thus scales well to large batch sizes.

Inspired by the Local Penalisation approach (LP) in synchronous BO (González et al., 2016), we approximate Eq. (6) for the case of  $c = 1$  as:

$$x_j = \arg \max_{x \in \mathcal{X}} \left\{ \alpha(x \mid \mathcal{D}_{s_-}) \prod_{i=1}^{k-1} \phi(x \mid x_i, \mathcal{D}_{s_-}) \right\}, \quad (7)$$

where  $\phi(x \mid x_i, \mathcal{D}_{s_-})$  is the penaliser function centred at the busy locations  $\{x_i\}_{i=1}^{k-1}$ . In the following subsections, we design effective penaliser functions by harnessing the Lipschitz properties of the function and its GP posterior. To simplify notation, we denote  $\phi(x \mid x_i, \mathcal{D}_{s_-})$  as  $\phi(x \mid x_i)$  and  $\alpha(x \mid \mathcal{D}_{s_-})$  as  $\alpha(x)$  in the remainder of the section.

### 5.1. Hard Local Penaliser

Assume the unknown objective function is Lipschitz continuous with constant  $L$  and has a global minimum value  $f(x^*) = M$  and  $x_j$  is a busy task,

$$|f(x_j) - M| \leq L\|x_j - x^*\|. \quad (8)$$

This implies  $x^*$  cannot lie within the spherical region centred on  $x_j$  with radius  $r_j = \frac{f(x_j) - M}{L}$ :

$$\mathbb{S}(x_j, r_j) = \mathcal{X} \{x \in \mathcal{X} : \|x - x_j\| \leq r_j\}. \quad (9)$$

If  $x_j$  is still under evaluation by a worker, there is no need for any further selections inside  $\mathbb{S}(x_j, r_j)$ .

Given that  $f(x_j) \sim \mathcal{N}(\mu(x_j), \sigma^2(x_j))$  and thus  $\mathbb{E}(r_j) = \frac{|\mu(x_j) - M|}{L}$ , applying Hoeffding's inequality for all  $\epsilon > 0$  (Jalali et al., 2013) gives

$$P(r_j > \mathbb{E}(r_j) + \epsilon) \leq \exp\left(-\frac{2\epsilon^2 L^2}{\sigma(x_j)^2}\right), \quad (10)$$

which implies there is a high probability (around 99%) that  $r_j \leq \frac{|\mu(x_j) - M|}{L} + 1.5 \frac{\sigma(x_j)}{L}$ .

The penalisation function  $\phi(x | x_j)$  should incorporate this belief to guide the selection of the next asynchronous batch point by reducing the value of the acquisition function at locations  $\{x \in \mathbb{S}(x_j, r_j)\}$ . A valid penaliser should possess the several properties:

- the penalisation region shrinks as the expected function value at  $x_j$  gets close to the global minimum (i.e. small  $|\mu(x_j) - M|$ ) (González et al., 2016);
- the penalisation region shrinks as  $L$  increases (González et al., 2016);
- the extent of penalisation on  $\alpha(x)$  increases as  $x$  gets closer to  $x_j$  with  $\alpha(x_j) = 0$  if  $\alpha(x) \geq 0$  for all  $x \in \mathcal{X}$ .

The Local Penaliser (LP) in (González et al., 2016) fulfils the first two properties but not the final one which we believe is crucial. Thus, directly using it for the asynchronous case makes the algorithm vulnerable to redundant sampling as illustrated in Fig. 2. In view of this limitation, we propose a simple yet effective Hard Local Penaliser (HLP) which satisfies all three conditions

$$\phi(x | x_j) = \min\left\{\frac{\|x - x_j\|}{\mathbb{E}(r_j) + \gamma \frac{\sigma(x_j)}{L}}, 1\right\}, \quad (11)$$

where  $\gamma$  is a constant.

The above expression can be made differentiable by the approximation:

$$\hat{\phi}(x | x_j) = \left[\left(\frac{\|x - x_j\|}{\mathbb{E}(r_j) + \gamma \frac{\sigma(x_j)}{L}}\right)^p + 1^p\right]^{1/p}, \quad (12)$$

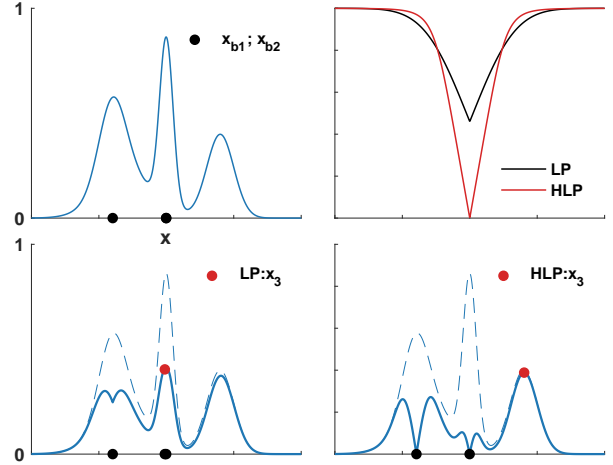


Figure 2. Illustration of asynchronous batch selection by naïve LP and HLP. The top left plot shows the acquisition function  $\alpha(x)$  and the locations (i.e.  $x_{b1}$  and  $x_{b2}$  denoted in black dots) under evaluation by busy workers. The top right plot shows the shapes of two penalisers at the busy location  $x_{b1}$ . Their respective penalisation effects on  $\alpha(x)$  at  $x_{b1}$  and  $x_{b2}$  as well as the new batch point  $x_3$  to be assigned to the available worker are shown in the subplots that follow, LP on the left and HLP on the right.

with  $\hat{\phi}(x | x_j) \rightarrow \phi(x | x_j)$  as  $p \rightarrow -\infty$ .

In addition, the global optimum  $M$  is unknown in practice and is usually approximated by the best function value observed  $\hat{M} = \min\{f(x_i)\}_i^n$  (González et al., 2016). This approximation tends to lead to underestimation of  $\mu(x_j) - M$  and thus  $\mathbb{E}(r_j)$ , reducing the extent of the penalisation at  $x_j$  and in the region nearby. HLP mitigates this effect by penalising significantly harder than the penaliser proposed by González et al. (2016), and maximally at  $x_j$  ( $\alpha(x_j) = 0$ ). Thus, our method is less affected by over-estimation of the global minimum  $\hat{M} > M$ .

### 5.2. Local Estimated Lipschitz constants

In BO, the global Lipschitz constant  $L$  of the objective function is unknown. Assuming the true objective function  $f$  is a draw from its GP surrogate model, we can approximate  $L$  with  $\hat{L} = \max_{x \in \mathcal{X}} \|\mu_{\nabla}(x)\|$  where  $\mu_{\nabla}(x)$  is the posterior mean of the derivative GP (González et al., 2016). However, using the estimated global Lipschitz constant  $\hat{L}$  to design the shape of the penalisers at all busy locations in the batch may not be optimal. Consider the case where a point in an unexplored region is still under evaluation. If  $\hat{L}$  is large, then the penaliser's radius will be small and we will end up selecting multiple points in the same unexplored region, which is undesirable.

Therefore, we propose to use a separate Lipschitz constant, which is locally estimated, for each busy location. Here,



“locality” is encoded in our choice of kernel and its hyperparameters, e.g. via the lengthscale parameter in the Matérn class of kernels. The use of local Lipschitz constants will enhance the efficiency of exploration because they allow the penaliser to create larger exclusion zones in areas in which we are very uncertain (the surrogate model is near its prior or has low curvature) and smaller penalisation zones in interesting, high-variability, areas. This insight is also corroborated in (Blaas et al., 2019).

We demonstrate the different effects of using approximate global and local Lipschitz constants with a qualitative example. In Fig. 3a, the estimated global Lipschitz constant is used for penalisation at both busy locations  $x_{b1} = -1$  and  $x_{b2} = 1$  (denoted as black dots). The relatively large value of the global Lipschitz constant ( $\hat{L}_{b1} = \hat{L}_{b2} = \hat{L} = 3.47$ ) due to the high curvature of the surrogate in the central region leads to a small penalisation zone around the two busy locations at the boundary. This causes the algorithm to miss the informative region in the centre and instead revisit the region near  $x_{b1}$  to choose the new point in the asynchronous batch. On the other hand, in Fig. 3b, the use of a locally estimated Lipschitz constant allows us to penalise a larger zone around points where the surrogate is relatively flat ( $\hat{L}_{b1} = 0.712$  for  $x_{b1}$ ), while still penalising smaller regions where there is higher variability ( $\hat{L}_3 = 3.45$  at  $x_3$ ).

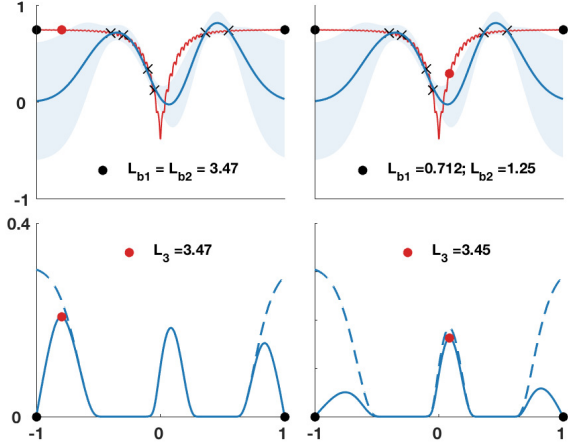
In our experiments we used a Matérn-52 kernel and defined the local region for evaluating the Lipschitz constant for a batch point  $x_j$  to be a hypercube centred on  $x_j$  with the length of the each side equal to the lengthscale corresponding to that input dimension.

In summary, we propose a new class of asynchronous BO methods, Penalisation Locally for Asynchronous Bayesian Optimisation Of K workers (PLAyBOOK), which uses analytic penaliser functions to prevent redundant sampling at or near the busy locations in the batch and encourage desirably explorative searching behaviour. We differentiate between PLAyBOOK-L, which uses a naïve Local penaliser, PLAyBOOK-H, that uses the HLP penaliser, as well as their variations with locally estimated Lipschitz constants, PLAyBOOK-LL and PLAyBOOK-HL.

## 6. Experimental evaluation

We begin our empirical investigations by performing a head-to-head comparison of synchronous and asynchronous BO methods, to test the intuitions described in Section 4. We specifically look at optimisation performance for asynchronous and synchronous variants of the parallel BO methods measured over time and number of evaluations, and we show empirically that asynchronous is preferable over synchronous BO on both counts.

We then experiment with our proposed asynchronous meth-



(a) Penalisation with global L (b) Penalisation with local L

Figure 3. Different penalisation effects on  $\alpha(x)$  of using a single global Lipschitz constant compared to local Lipschitz constants. The top plots in both (a) and (b) show the true objective function (red line), six observed points (black crosses), the GP posterior mean (black line) and variance (blue shade), the two busy locations (black dots) and the next query point (red dot) selected by using the HLP with global and local Lipschitz constants respectively. The plots in (a) show the penalisation effect on busy locations using the same global Lipschitz constant while those in (b) show the effect of using local Lipschitz constants. It is clear that penalising the busy locations based on local Lipschitz constants allows the algorithm to capture the informative peak at the central region while selection based on the single global Lipschitz constant leads us to revisit the flat region near the boundary due to insufficient penalisation at  $x_1$ .

ods (PLAyBOOK-L, PLAyBOOK-H, PLAyBOOK-LL and PLAyBOOK-HL) on a number of benchmark test functions as well as a real-world expensive optimisation task. Our methods are compared against the state-of-the-art asynchronous BO methods, Thompson sampling (TS) (Kandasamy et al., 2018), as well as the Kriging Believer heuristic method (KB) (Ginsbourger et al., 2010) applied asynchronously.

For all the benchmark functions, we measure the log of the simple regret  $R$ , which is the difference between the true minimum value  $f(x^*)$  and the best value found by the BO method:

$$\log(R) = \log \left| f(x^*) - \min_{i=1, \dots, n} f(x_i) \right|. \quad (13)$$

### 6.1. Implementation details

To ensure a fair comparison, we implemented all methods in Python using the same packages<sup>1</sup>.

<sup>1</sup> Implementation available at <https://github.com/a5a/asynchronous-BO>

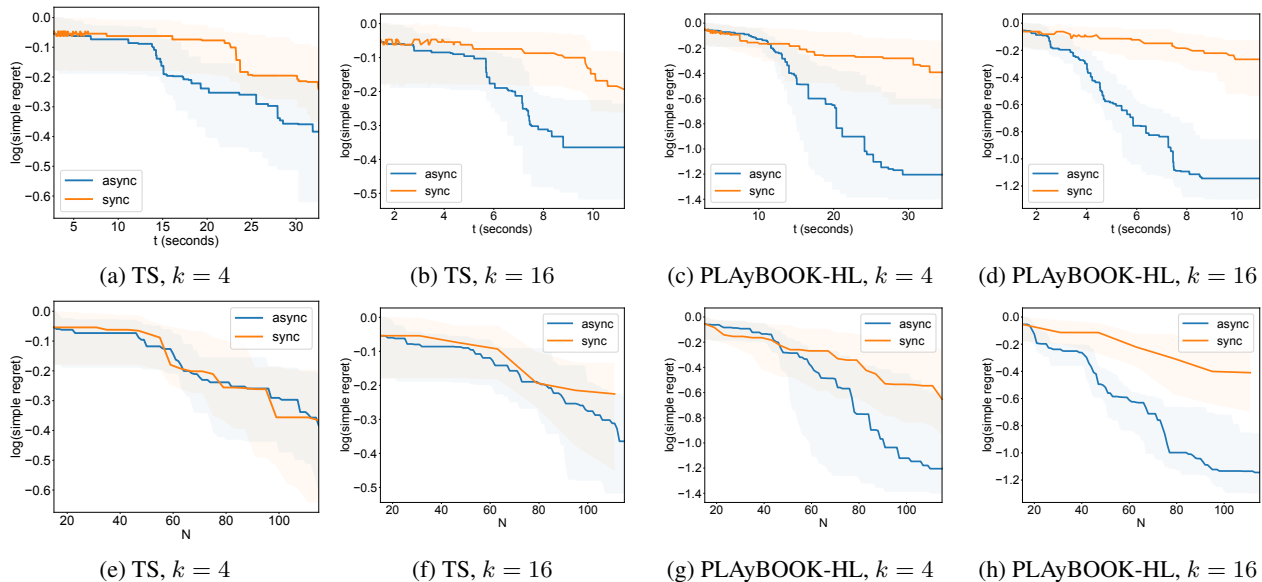


Figure 4. A head-to-head comparison of synchronous (orange) vs asynchronous (blue) versions of a parallel BO method. The median (solid line) and quartiles (shaded region) of the regret for optimising ack-5D for 30 random initialisations are shown. The top row shows regret vs evaluation time and the bottom row shows regret vs number of evaluations. Notice how asynchronous methods in the top row outperform their synchronous counterparts in terms of evaluation time. Note also how asynchronous methods in the bottom row outperform their synchronous counterparts in terms of sample efficiency, too.

In all experiments, we used a zero-mean Gaussian process surrogate model with a Matérn-52 kernel with ARD. We optimised the kernel and likelihood hyperparameters by maximising the log marginal likelihood. For the benchmark test functions, we fixed the noise variance to  $\sigma^2 = 10^{-6}$  and started with  $3 * d$  random initial observations. Each experiment was repeated with 30 different random initialisations and the input domains for all experiments were scaled to  $[-1, 1]^d$ .

All methods except TS used UCB as the acquisition function  $\alpha(x)$ . For our PLAyBOOK-H and PLAyBOOK-HL, we choose  $\gamma = 1$  and  $p = -5$  in the HLP (Eq. (12)). For TS, we use 10,000 sample points for each batch point selection. For the other methods, we evaluate  $\alpha(x)$  at 3,000 random locations and then choose the best one after locally optimising the best 5 samples for a small number of local optimisation steps.

We evaluate the performance of the different batch BO strategies using popular global optimisation test functions<sup>2</sup>. We show results for the Eggholder function defined on  $\mathbb{R}^2$  (egg-2D), the Ackley function defined on  $\mathbb{R}^5$  and the Michalewicz function defined on  $\mathbb{R}^{10}$  (mic-10D). Results for experiments on different example tasks can be found in Sections 2 and 3 in the supplementary materials.

<sup>2</sup>Details for these and other challenging global optimisation test functions can be found at <https://www.sfu.ca/~ssurjano/optimization.html>

## 6.2. Synchronous vs asynchronous BO

In this section we address the question of choosing between asynchronous and synchronous BO. In order to investigate their relative merits, we compared asynchronous and synchronous BO methods’ performance as a function of wall-clock time and number of evaluations.

### 6.2.1. EVALUATION TIME

In order to facilitate this comparison, we needed to inject a measure of runtime for different tasks, as the test functions can be evaluated instantaneously. We followed the procedure proposed in Kandasamy et al. (2018) to sample an evaluation time for each task so as to simulate the asynchronous setting. We chose to use a half-normal distribution with scale parameter  $\sigma = \sqrt{\pi/2}$ , which gives us a distribution of runtime values with mean at 1.

Results on the ack-5D task are shown in Figs. 4(a)-(d). Due to space constraints, results for further experiments can be found in Section 2 of the supplementary materials. We know that asynchronous BO has the advantage over synchronous BO in terms of utilisation of resources, as shown qualitatively in Fig. 1, simply due to the fact that any available worker is not required to wait for all evaluations in the batch to finish before moving on. Therefore, given the same time budget, a greater number of evaluations can be taken in the asynchronous setting than in the synchronous setting, which, as confirmed by our experiments, translates

to faster optimisation of  $f$  in terms of the total (wall-clock) time spent evaluating tasks.

### 6.2.2. NUMBER OF EVALUATIONS

A more interesting question to answer is whether asynchronous BO methods are really less data efficient than synchronous BO methods as discussed in Section 4. Figs. 4(e)-(h) show a subset of the experiments we conducted. More results can be found in Section 2 in the supplementary materials.

An unexpected yet interesting behaviour we note is that as  $k$  increases, the PLAyBOOK methods tend to clearly outperform their respective synchronous counterparts even in terms of sample efficiency. This observation runs counter to the guidance provided in Kandasamy et al. (2018) and such behaviour is less evident for the other two batch methods, TS and KB.

We think this observation may be explained by the difference in nature between the PLAyBOOK and TS/KB: in the case of TS we rely on stochasticity in sampling, and in KB we are re-computing the posterior variance and  $\alpha(x)$  each time a batch point is selected. The penalisation-based methods, on the other hand, simply down-weight the acquisition function, and in the synchronous case these penalisers coincide with the high-value regions of the acquisition function. This means that unless the acquisition function has a large number of spaced-out peaks, we will quickly be left without high-utility locations to choose new batch points from.

This seems to be the reason for the superior performance of asynchronous PLAyBOOK methods over their synchronous variants because they benefit from the fact that the busy locations being penalised do not necessarily coincide with the peaks in  $\alpha(x)$ , as the surrogate used to compute  $\alpha(x)$  is more informed than the one used to decide the locations of the busy locations previously. This means that points with high utilities are more likely to be preserved.

Taking into account the fact that the asynchronous PLAyBOOK methods tend to perform at least equally well, if not significantly better than their synchronous variants on both time and efficiency, and that the asynchronous PLAyBOOK methods gain more advantage over synchronous ones as the batch size increases, we believe that this points to the fact that penalisation-based methods are inherently better suited as asynchronous methods. Hence, for users that are running parallel BO and have selected LP, we recommend they consider running PLAyBOOK instead due to its attractive benefits.

## 6.3. Asynchronous parallel BO

Now that we have strengthened the appeal of asynchronous BO, we turn to evaluating PLAyBOOK against existing

asynchronous BO methods.

### 6.3.1. SYNTHETIC EXPERIMENTS

We ran PLAyBOOK and competing asynchronous BO methods on the global optimisation test functions described in Section 6.1. The results are shown in Fig. 5, and more results on different optimisation problems are provided in Section 3 in the supplementary materials.

On the global optimisation test functions we noted that in most cases PLAyBOOK outperforms the alternative asynchronous methods TS and KB. The TS algorithm performed poorly on this test, which we believe is caused by the fact that TS relies heavily on the surrogate’s uncertainty to explore new regions.

PLAyBOOK methods show strong performance, achieving better optimisation performance than both TS and KB baselines.

### 6.3.2. REAL-WORLD OPTIMISATION

We further experimented on a real-world application of tuning the hyperparameters of a 6-layer Convolutional Neural Network (CNN)<sup>3</sup> for an image classification task on CIFAR10 dataset (Krizhevsky, 2009). The 9 hyperparameters that we optimise with BO are the learning rate and momentum for the stochastic gradient descent training algorithm, the batch size used and the number of filters in each of the six convolutional layers. We trained the CNN on half of the training set for 20 epochs and each function evaluation returns the validation error of the model. We tested the use of  $k = 2$  and  $k = 4$  parallel workers to run this real-world experiment. The results are shown in Figs. 6a and 6b.

We can see that for both  $k = 2$  and  $k = 4$  parallel settings, all PLAyBOOK methods outperform the other asynchronous methods, TS and KB. In the case of  $k = 2$  (2 parallel processors), only one busy location is penalised in each batch so there is little gain from using a locally estimated Lipschitz constant. However, as the batch size increases to  $k = 4$ , we see that methods using estimated Lipschitz constants (PLAyBOOK-LL and PLAyBOOK-HL) show faster decrease in validation error than PLAyBOOK-L and PLAyBOOK-H with PLAyBOOK-LL demonstrating the best performance.

We then took the final configurations recommended by each asynchronous BO method in the  $k = 2$  and  $k = 4$  settings and retrained the CNN model on the full training set of 50K images for 80 epochs. The accuracy on the test set of 10K images achieved with the best model chosen by

<sup>3</sup>Follow the implementation in <https://blog.plon.io/tutorials/cifar-10-classification-using-keras-tutorial/>

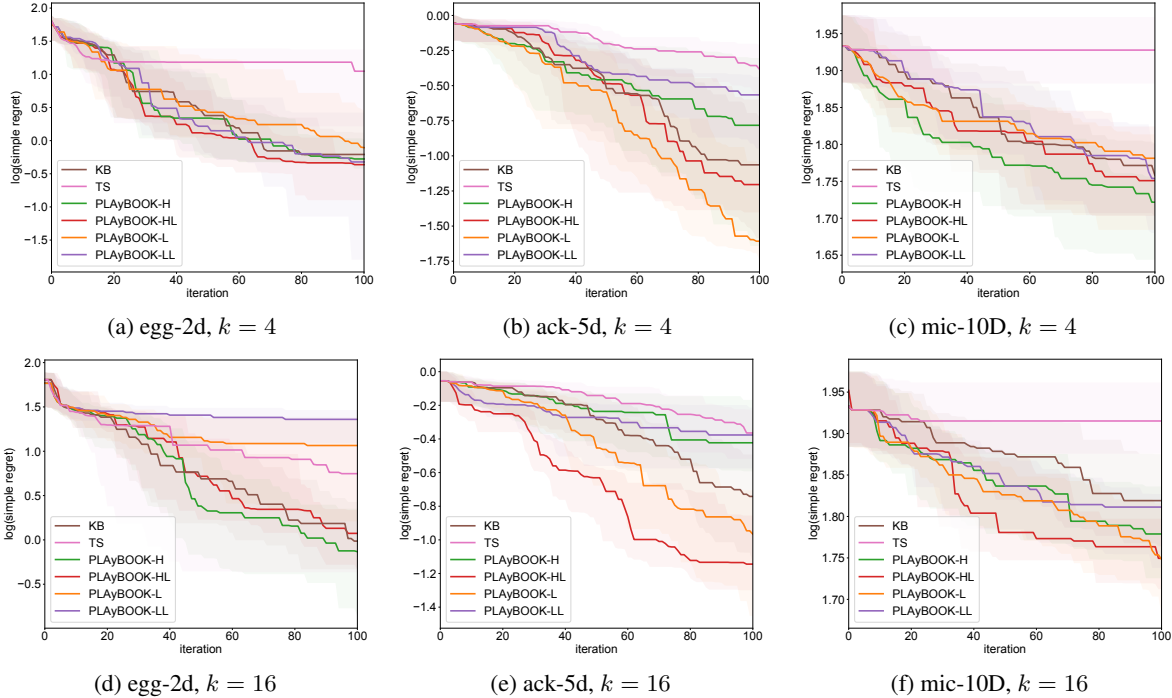


Figure 5. The median (solid line) and quartiles (shaded region) of the regret for different asynchronous BO methods on the global optimisation test functions for 30 random initialisations is shown. We can see that our proposed PLAYBOOK methods perform competitively, especially when we start choosing larger batch sizes.

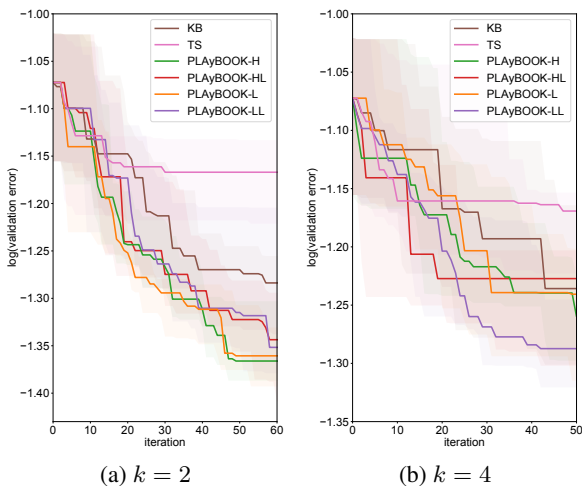


Figure 6. Asynchronous optimisation of 9 hyperparameters of a 6-layer CNN for image classification on the CIFAR10 dataset. The network is trained on half of the training set and evaluated on the second half. The objective being minimised is the classification accuracy on the validation set. PLAYBOOK outperforms both KB and TS in this expensive optimisation task.

each BO method is shown in Table 1. In both settings, our PLAYBOOK methods achieve superior performance over TS with PLAYBOOK-H providing the best test accuracy when

$k = 2$  and PLAYBOOK-LL doing the best when  $k = 4$ .

Table 1. Test accuracy (%) on CIFAR-10 after training the best model chosen by various asynchronous BO methods for 80 epochs

$k$	TS	KB	PLAYBOOK			
			L	H	LL	HL
2	81.0	83.9	84.7	<b>85.2</b>	84.1	84.9
4	81.2	82.8	82.5	83.8	<b>84.2</b>	83.0

## 7. Conclusions

We argue for the use of asynchronous (over synchronous) Bayesian optimisation (BO), and provide supporting empirical evidence. Additionally, we developed a new approach, PLAYBOOK, for asynchronous BO, based on penalisation of the acquisition function using information about tasks that are still under evaluation. Empirical evaluation on synthetic functions and a real-world optimisation task showed that PLAYBOOK improves upon the state of the art. Finally, we demonstrate that, for penalisation-based batch BO, PLAYBOOK’s asynchronous BO is more efficient than synchronous BO in both wall-clock time and the number of samples.



## Acknowledgements

We thank our colleagues at the Machine Learning Research Group at the University of Oxford, especially Edward Wagstaff, for providing discussions that assisted the research. We would also like to express our gratitude to our anonymous reviewers for their valuable comments and feedback.

Computational resources were supported by Arcus HTC and JADE HPC at the University of Oxford and Hartree national computing facilities, UK.

## References

- Azimi, J., Fern, A., and Fern, X. Z. Batch Bayesian optimization via simulation matching. In *Advances in Neural Information Processing Systems*, pp. 109–117, 2010.
- Blaas, A., Manzano, J. M., Limon, D., and Calliess, J. Localised kinky inference. In *Proceedings of the European Control Conference*, 2019.
- Brochu, E., Cora, V. M., and De Freitas, N. A tutorial on Bayesian optimization of expensive cost functions, with application to active user modeling and hierarchical reinforcement learning. *arXiv preprint arXiv:1012.2599*, 2010.
- Chen, Y., Huang, A., Wang, Z., Antonoglou, I., Schrittwieser, J., Silver, D., and de Freitas, N. Bayesian optimization in AlphaGo. *arXiv preprint arXiv:1812.06855*, 2018.
- Contal, E., Buffoni, D., Robicquet, A., and Vayatis, N. Parallel Gaussian process optimization with Upper Confidence Bound and Pure Exploration. In *Joint European Conference on Machine Learning and Knowledge Discovery in Databases*, pp. 225–240. Springer, 2013.
- Desautels, T., Krause, A., and Burdick, J. W. Parallelizing exploration-exploitation tradeoffs in Gaussian process bandit optimization. *The Journal of Machine Learning Research*, 15(1):3873–3923, 2014.
- Ginsbourger, D., Le Riche, R., and Carraro, L. A multi-points criterion for deterministic parallel global optimization based on Gaussian processes. 2008.
- Ginsbourger, D., Le Riche, R., and Carraro, L. Kriging is well-suited to parallelize optimization. In *Computational intelligence in expensive optimization problems*, pp. 131–162. Springer, 2010.
- Ginsbourger, D., Janusevskis, J., and Le Riche, R. Dealing with asynchronicity in parallel Gaussian process based global optimization. In *4th International Conference of the ERCIM WG on computing & statistics (ERCIM’11)*, 2011.
- González, J., Dai, Z., Hennig, P., and Lawrence, N. Batch Bayesian optimization via local penalization. In *Artificial Intelligence and Statistics*, pp. 648–657, 2016.
- Hennig, P. and Schuler, C. J. Entropy search for information-efficient global optimization. *Journal of Machine Learning Research*, 13(Jun):1809–1837, 2012.
- Hernández-Lobato, J. M., Hoffman, M. W., and Ghahramani, Z. Predictive entropy search for efficient global optimization of black-box functions. In *Advances in neural information processing systems*, pp. 918–926, 2014.
- Hernández-Lobato, J. M., Requeima, J., Pyzer-Knapp, E. O., and Aspuru-Guzik, A. Parallel and distributed Thompson sampling for large-scale accelerated exploration of chemical space. In *International Conference on Machine Learning (ICML)*, 2017.
- Jalali, A., Azimi, J., Fern, X., and Zhang, R. A Lipschitz exploration-exploitation scheme for Bayesian optimization. In *Joint European Conference on Machine Learning and Knowledge Discovery in Databases*, pp. 210–224. Springer, 2013.
- Jones, D. R., Schonlau, M., and Welch, W. J. Efficient global optimization of expensive black-box functions. *Journal of Global optimization*, 13(4):455–492, 1998.
- Kandasamy, K., Krishnamurthy, A., Schneider, J., and Póczos, B. Parallelised Bayesian optimisation via Thompson sampling. In *International Conference on Artificial Intelligence and Statistics*, pp. 133–142, 2018.
- Kathuria, T., Deshpande, A., and Kohli, P. Batched Gaussian process bandit optimization via determinantal point processes. In *Advances in Neural Information Processing Systems*, pp. 4206–4214, 2016.
- Krizhevsky, A. Learning multiple layers of features from tiny images. Technical report, Citeseer, 2009.
- Kushner, H. J. A new method of locating the maximum point of an arbitrary multipeak curve in the presence of noise. *Journal of Basic Engineering*, 86(1):97–106, 1964.
- Rasmussen, C. E. and Williams, C. K. *Gaussian processes for machine learning*, volume 1. MIT press Cambridge, 2006.
- Ru, B., McLeod, M., Granzol, D., and Osborne, M. A. Fast information-theoretic Bayesian optimisation. In *International Conference on Machine Learning (ICML)*, 2018.
- Shah, A. and Ghahramani, Z. Parallel predictive entropy search for batch global optimization of expensive objective functions. In *Advances in Neural Information Processing Systems*, pp. 3330–3338, 2015.

- Srinivas, N., Krause, A., Kakade, S. M., and Seeger, M. Gaussian process optimization in the bandit setting: No regret and experimental design. In *International Conference on Machine Learning (ICML)*, 2010.
- Wang, J., Clark, S. C., Liu, E., and Frazier, P. I. Parallel Bayesian global optimization of expensive functions. *arXiv preprint arXiv:1602.05149*, 2016.
- Wang, Z. and Jegelka, S. Max-value entropy search for efficient Bayesian optimization. In *International Conference on Machine Learning (ICML)*, 2017.
- Wu, J. and Frazier, P. The parallel knowledge gradient method for batch Bayesian optimization. In *Advances in Neural Information Processing Systems*, pp. 3126–3134, 2016.

---

# Supplementary material

---

## 1. Summary of experimental tasks

As mentioned in the main text, we conducted empirical evaluations on a large number of synthetic test problems:

- The tasks mat-2 and mat-6 refer to functions drawn from a Gaussian process(GP) with Matérn-5/2 kernel in  $\mathbb{R}^2$  and  $\mathbb{R}^6$  respectively.
- The global optimisation tasks<sup>4</sup> that we considered are the Ackley function defined on  $\mathbb{R}^5$  and  $\mathbb{R}^{10}$  (ack-5 and ack-10), the Michalewicz function defined on  $\mathbb{R}^5$  and  $\mathbb{R}^{10}$  (mic-5 and mic-10) and the Eggholder function in  $\mathbb{R}^2$  (egg-2).
- We also selected a robot pushing simulation experiment, which was first explored in a BO context by Wang & Jegelka (2017). Here the task is to learn the correct pushing action to minimise the distance of the robot to a goal. The problem has 4 inputs: the robot’s location  $(r_x, r_y)$ , the angle of the pushing force  $r_\theta$  and the pushing duration  $t_r$ . We used the input space suggested by Wang & Jegelka (2017).

## 2. Asynchronous vs. synchronous parallel BO

Similar to Fig. 4 in the main text, Figs. 7 and 8 show head-to-head comparisons of synchronous and asynchronous methods, here on the ack-10 task.

## 3. Asynchronous BO

We conducted a large number of experiments testing the different approaches for asynchronous BO. We computed the mean and standard deviation of the log of the simple regret across 30 random initialisations (see Eq. 13 in the main text for the definition). Tables 2, 3 and 4 show the results after 50, 75 and 100 asynchronous BO steps respectively.

Across all of these experiments, we can see that PLAyBOOK is performing competitively, making it an attractive choice for asynchronous BO problems.

---

<sup>4</sup>Details for these and other challenging global optimisation test functions can be found at <https://www.sfu.ca/~ssurjano/optimization.html>

k	Task	KB	TS	PLAYBOOK			
				L	LL	H	HL
2	ack-10	-0.30 (0.16)	-0.01 (0.03)	-0.23 (0.15)	<b>-0.37 (0.25)</b>	-0.32 (0.18)	-0.27 (0.18)
	ack-5	-0.55 (0.39)	-0.22 (0.20)	<b>-0.85 (0.52)</b>	-0.52 (0.40)	-0.64 (0.39)	-0.71 (0.48)
	egg-2	0.28 (0.72)	0.89 (0.92)	-0.12 (1.26)	-0.05 (1.03)	<b>-0.44 (2.13)</b>	-0.31 (1.62)
	mat-2	0.81 (0.30)	1.05 (0.26)	<b>0.78 (0.28)</b>	0.82 (0.26)	0.81 (0.21)	0.89 (0.20)
	mat-6	1.02 (0.16)	1.13 (0.14)	<b>0.85 (0.43)</b>	0.92 (0.33)	0.88 (0.26)	0.86 (0.31)
	mic-10	1.84 (0.08)	1.92 (0.07)	<b>1.78 (0.11)</b>	1.80 (0.09)	1.82 (0.11)	1.83 (0.10)
	mic-5	0.71 (0.28)	1.02 (0.13)	0.67 (0.27)	<b>0.66 (0.26)</b>	0.69 (0.33)	0.87 (0.16)
nrobot-4	-0.71 (1.05)	-0.52 (1.21)	-0.88 (0.91)	-0.78 (0.86)	<b>-0.89 (0.69)</b>	-0.87 (0.91)	
4	ack-10	-0.29 (0.17)	-0.01 (0.03)	-0.26 (0.16)	-0.32 (0.17)	-0.25 (0.14)	<b>-0.34 (0.18)</b>
	ack-5	-0.54 (0.36)	-0.21 (0.13)	-0.66 (0.45)	-0.41 (0.27)	-0.53 (0.41)	<b>-0.71 (0.52)</b>
	egg-2	0.19 (1.06)	0.79 (0.92)	0.53 (0.91)	0.23 (0.98)	0.29 (0.86)	<b>-0.06 (1.26)</b>
	mat-2	<b>0.77 (0.30)</b>	0.98 (0.37)	0.94 (0.22)	1.01 (0.28)	0.82 (0.25)	0.87 (0.22)
	mat-6	1.06 (0.17)	1.13 (0.05)	0.99 (0.18)	1.01 (0.26)	0.95 (0.23)	<b>0.94 (0.20)</b>
	mic-10	1.82 (0.11)	1.92 (0.07)	1.82 (0.08)	1.83 (0.08)	<b>1.78 (0.09)</b>	1.80 (0.08)
	mic-5	<b>0.66 (0.28)</b>	1.01 (0.16)	0.78 (0.23)	0.87 (0.19)	0.76 (0.20)	0.82 (0.33)
nrobot-4	-0.67 (1.00)	-0.39 (1.04)	<b>-1.01 (0.94)</b>	-0.94 (0.97)	-0.75 (0.70)	-0.63 (0.79)	
6	ack-10	-0.24 (0.19)	-0.01 (0.04)	-0.29 (0.15)	-0.25 (0.14)	-0.20 (0.14)	<b>-0.31 (0.16)</b>
	ack-5	-0.51 (0.28)	-0.20 (0.20)	<b>-0.54 (0.40)</b>	-0.27 (0.18)	-0.35 (0.24)	-0.49 (0.27)
	egg-2	0.37 (1.05)	0.78 (0.88)	0.71 (0.83)	0.77 (0.82)	<b>0.07 (1.25)</b>	0.32 (1.11)
	mat-2	0.85 (0.25)	1.04 (0.19)	0.98 (0.34)	1.06 (0.23)	<b>0.84 (0.23)</b>	0.85 (0.25)
	mat-6	1.01 (0.17)	1.07 (0.18)	<b>0.95 (0.28)</b>	1.02 (0.28)	1.03 (0.16)	0.99 (0.24)
	mic-10	1.84 (0.08)	1.92 (0.07)	1.84 (0.08)	1.81 (0.08)	1.84 (0.08)	<b>1.80 (0.09)</b>
	mic-5	<b>0.76 (0.21)</b>	1.04 (0.15)	0.84 (0.23)	0.89 (0.24)	0.88 (0.19)	0.87 (0.20)
nrobot-4	-0.58 (0.96)	-0.22 (0.95)	<b>-0.69 (1.04)</b>	-0.47 (0.85)	-0.63 (1.02)	-0.51 (0.99)	
8	ack-10	-0.23 (0.17)	-0.01 (0.03)	-0.26 (0.17)	-0.34 (0.15)	-0.17 (0.11)	<b>-0.40 (0.14)</b>
	ack-5	-0.44 (0.27)	-0.19 (0.14)	-0.65 (0.40)	-0.33 (0.21)	-0.38 (0.30)	<b>-0.68 (0.37)</b>
	egg-2	0.31 (0.93)	0.65 (0.92)	0.60 (1.20)	0.93 (0.77)	0.42 (0.61)	<b>0.17 (1.05)</b>
	mat-2	0.80 (0.22)	0.93 (0.26)	0.81 (0.44)	1.09 (0.20)	0.87 (0.27)	<b>0.79 (0.30)</b>
	mat-6	<b>1.01 (0.19)</b>	1.13 (0.06)	1.03 (0.17)	1.02 (0.22)	1.03 (0.15)	1.03 (0.20)
	mic-10	1.84 (0.09)	1.91 (0.07)	1.82 (0.08)	1.81 (0.10)	1.80 (0.13)	<b>1.78 (0.08)</b>
	mic-5	0.70 (0.33)	1.02 (0.20)	<b>0.68 (0.32)</b>	0.79 (0.25)	0.73 (0.32)	0.69 (0.32)
nrobot-4	-0.61 (0.78)	-0.20 (0.96)	<b>-0.94 (0.92)</b>	-0.62 (1.14)	-0.76 (1.11)	-0.39 (0.73)	
16	ack-10	-0.13 (0.08)	-0.02 (0.04)	-0.24 (0.13)	-0.24 (0.13)	-0.22 (0.10)	<b>-0.44 (0.13)</b>
	ack-5	-0.36 (0.30)	-0.18 (0.16)	-0.49 (0.34)	-0.36 (0.24)	-0.28 (0.19)	<b>-0.73 (0.26)</b>
	egg-2	0.58 (0.73)	0.56 (1.10)	1.04 (0.51)	1.22 (0.50)	<b>0.30 (0.96)</b>	0.71 (0.53)
	mat-2	<b>0.82 (0.27)</b>	0.89 (0.24)	1.07 (0.17)	1.12 (0.20)	0.92 (0.31)	0.90 (0.31)
	mat-6	1.10 (0.05)	1.14 (0.03)	1.05 (0.14)	1.06 (0.21)	1.02 (0.26)	<b>1.00 (0.26)</b>
	mic-10	1.86 (0.08)	1.90 (0.07)	1.82 (0.07)	1.82 (0.09)	1.83 (0.08)	<b>1.79 (0.09)</b>
	mic-5	<b>0.81 (0.25)</b>	1.02 (0.19)	0.85 (0.21)	0.84 (0.23)	0.81 (0.22)	0.82 (0.25)
nrobot-4	-0.43 (0.94)	-0.22 (0.99)	<b>-0.78 (0.95)</b>	-0.14 (0.77)	-0.37 (0.80)	-0.40 (0.81)	

Table 2. Mean and standard deviation of the log(regret) after 50 steps of asynchronous BO.



k	Task	KB	TS	PLAYBOOK			
				L	LL	H	HL
2	ack-10	-0.43 (0.18)	-0.01 (0.03)	-0.48 (0.27)	<b>-0.58 (0.26)</b>	-0.55 (0.32)	-0.45 (0.28)
	ack-5	-0.91 (0.56)	-0.32 (0.22)	<b>-1.15 (0.58)</b>	-0.76 (0.50)	-1.03 (0.52)	-0.92 (0.51)
	egg-2	-0.12 (0.92)	0.87 (0.91)	-0.59 (1.16)	<b>-1.13 (2.14)</b>	-0.81 (1.99)	-0.82 (1.68)
	mat-2	0.80 (0.30)	1.05 (0.27)	<b>0.76 (0.28)</b>	0.81 (0.26)	0.81 (0.21)	0.87 (0.20)
	mat-6	0.95 (0.21)	1.17 (0.14)	<b>0.74 (0.53)</b>	0.87 (0.31)	0.84 (0.34)	0.89 (0.29)
	mic-10	1.79 (0.12)	1.92 (0.07)	<b>1.75 (0.11)</b>	1.76 (0.14)	1.79 (0.12)	1.79 (0.13)
	mic-5	<b>0.52 (0.42)</b>	0.97 (0.17)	0.61 (0.29)	0.56 (0.24)	0.57 (0.37)	0.73 (0.28)
nrobot-4	-1.06 (1.08)	-0.83 (1.18)	-1.20 (0.86)	<b>-1.31 (0.75)</b>	-1.24 (0.78)	-1.29 (0.80)	
4	ack-10	<b>-0.52 (0.21)</b>	-0.01 (0.03)	-0.51 (0.27)	-0.42 (0.19)	-0.46 (0.22)	-0.50 (0.22)
	ack-5	-0.83 (0.48)	-0.31 (0.23)	<b>-1.10 (0.53)</b>	-0.57 (0.33)	-0.75 (0.62)	-0.90 (0.54)
	egg-2	-0.19 (0.87)	0.69 (1.13)	0.16 (1.70)	-0.81 (2.55)	-0.23 (1.10)	<b>-0.89 (2.48)</b>
	mat-2	<b>0.75 (0.29)</b>	0.98 (0.37)	0.93 (0.22)	1.01 (0.28)	0.80 (0.25)	0.85 (0.22)
	mat-6	0.97 (0.27)	1.18 (0.06)	0.95 (0.23)	1.02 (0.24)	<b>0.86 (0.28)</b>	0.87 (0.30)
	mic-10	1.77 (0.12)	1.92 (0.07)	1.77 (0.09)	1.78 (0.09)	<b>1.74 (0.09)</b>	1.77 (0.10)
	mic-5	<b>0.56 (0.30)</b>	0.97 (0.14)	0.69 (0.25)	0.76 (0.19)	0.63 (0.22)	0.67 (0.34)
nrobot-4	-0.92 (0.95)	-1.01 (1.31)	<b>-1.51 (0.88)</b>	-1.23 (0.89)	-1.07 (0.68)	-1.04 (0.79)	
6	ack-10	-0.41 (0.22)	-0.01 (0.04)	<b>-0.50 (0.26)</b>	-0.30 (0.15)	-0.32 (0.18)	-0.38 (0.19)
	ack-5	-0.83 (0.46)	-0.32 (0.23)	<b>-0.86 (0.54)</b>	-0.36 (0.23)	-0.52 (0.31)	-0.76 (0.37)
	egg-2	0.19 (1.00)	0.64 (1.14)	0.56 (0.93)	0.75 (0.84)	<b>-0.34 (1.48)</b>	-0.21 (1.03)
	mat-2	<b>0.82 (0.26)</b>	1.03 (0.20)	0.98 (0.34)	1.06 (0.23)	0.82 (0.22)	0.84 (0.25)
	mat-6	0.92 (0.25)	1.14 (0.17)	<b>0.86 (0.36)</b>	1.08 (0.25)	0.95 (0.28)	0.94 (0.26)
	mic-10	1.81 (0.08)	1.92 (0.07)	1.81 (0.08)	1.79 (0.09)	1.80 (0.10)	<b>1.78 (0.10)</b>
	mic-5	<b>0.63 (0.28)</b>	1.00 (0.14)	0.74 (0.29)	0.82 (0.22)	0.76 (0.26)	0.69 (0.33)
nrobot-4	-1.02 (0.88)	-0.73 (1.20)	-0.99 (1.04)	-0.78 (0.96)	<b>-1.04 (1.02)</b>	-1.02 (0.95)	
8	ack-10	-0.44 (0.21)	-0.01 (0.03)	-0.47 (0.21)	-0.40 (0.20)	-0.28 (0.17)	<b>-0.52 (0.16)</b>
	ack-5	-0.77 (0.40)	-0.33 (0.20)	<b>-1.04 (0.45)</b>	-0.39 (0.22)	-0.52 (0.41)	-0.92 (0.36)
	egg-2	<b>-0.11 (0.96)</b>	0.57 (1.00)	0.40 (1.22)	0.85 (0.84)	0.22 (0.51)	-0.05 (0.96)
	mat-2	0.78 (0.23)	0.91 (0.26)	0.81 (0.44)	1.09 (0.20)	0.82 (0.26)	<b>0.76 (0.30)</b>
	mat-6	0.95 (0.24)	1.18 (0.10)	0.97 (0.20)	1.10 (0.20)	<b>0.93 (0.25)</b>	0.97 (0.28)
	mic-10	1.80 (0.09)	1.91 (0.07)	<b>1.75 (0.09)</b>	1.78 (0.09)	1.78 (0.13)	1.76 (0.08)
	mic-5	0.58 (0.38)	0.98 (0.19)	0.59 (0.36)	0.70 (0.26)	0.61 (0.33)	<b>0.55 (0.53)</b>
nrobot-4	-0.92 (0.89)	-0.65 (1.01)	<b>-1.25 (0.82)</b>	-0.92 (1.08)	-1.07 (1.10)	-0.92 (0.88)	
16	ack-10	-0.27 (0.14)	-0.02 (0.04)	-0.43 (0.21)	-0.31 (0.20)	-0.31 (0.14)	<b>-0.54 (0.16)</b>
	ack-5	-0.55 (0.34)	-0.29 (0.19)	-0.77 (0.42)	-0.39 (0.25)	-0.39 (0.28)	<b>-0.94 (0.30)</b>
	egg-2	0.26 (0.74)	0.41 (1.18)	0.89 (0.63)	1.21 (0.50)	<b>-0.39 (1.81)</b>	0.42 (0.61)
	mat-2	<b>0.79 (0.27)</b>	0.88 (0.24)	1.07 (0.17)	1.12 (0.20)	0.87 (0.30)	0.86 (0.31)
	mat-6	1.03 (0.20)	1.20 (0.03)	0.95 (0.21)	1.08 (0.25)	<b>0.94 (0.26)</b>	0.96 (0.36)
	mic-10	1.83 (0.09)	1.90 (0.07)	1.79 (0.08)	1.79 (0.09)	1.79 (0.10)	<b>1.75 (0.13)</b>
	mic-5	<b>0.66 (0.27)</b>	0.95 (0.21)	0.77 (0.25)	0.73 (0.39)	0.75 (0.23)	0.75 (0.25)
nrobot-4	-0.72 (0.87)	-0.80 (1.24)	<b>-1.00 (1.01)</b>	-0.61 (0.95)	-0.72 (0.61)	-0.79 (0.78)	

Table 3. Mean and standard deviation of the log(regret) after 75 steps of asynchronous BO.

k	Task	KB	TS	PLAYBOOK			
				L	LL	H	HL
2	ack-10	-0.67 (0.27)	-0.01 (0.03)	-0.72 (0.34)	-0.73 (0.29)	<b>-0.80 (0.35)</b>	-0.58 (0.26)
	ack-5	-1.28 (0.70)	-0.35 (0.22)	<b>-1.49 (0.65)</b>	-0.95 (0.53)	-1.39 (0.62)	-1.08 (0.47)
	egg-2	-0.42 (1.62)	0.80 (0.92)	-1.10 (1.56)	<b>-1.58 (2.49)</b>	-1.54 (2.28)	-1.30 (2.01)
	mat-2	0.79 (0.30)	1.04 (0.25)	<b>0.76 (0.28)</b>	0.81 (0.26)	0.81 (0.21)	0.87 (0.19)
	mat-6	1.00 (0.21)	1.27 (0.17)	<b>0.93 (0.36)</b>	1.00 (0.31)	0.94 (0.26)	1.01 (0.27)
	mic-10	1.76 (0.13)	1.92 (0.07)	<b>1.72 (0.10)</b>	1.73 (0.13)	1.72 (0.13)	1.76 (0.12)
	mic-5	<b>0.39 (0.51)</b>	0.94 (0.18)	0.54 (0.31)	0.45 (0.24)	0.45 (0.36)	0.65 (0.28)
4	nrobot-4	-1.33 (1.02)	-1.12 (1.21)	-1.54 (0.84)	-1.51 (0.85)	-1.46 (0.74)	<b>-1.58 (0.78)</b>
	ack-10	<b>-0.72 (0.24)</b>	-0.01 (0.03)	-0.68 (0.28)	-0.54 (0.24)	-0.67 (0.24)	-0.56 (0.24)
	ack-5	-1.13 (0.59)	-0.41 (0.25)	<b>-1.46 (0.59)</b>	-0.68 (0.32)	-0.98 (0.73)	-1.04 (0.52)
	egg-2	-0.27 (0.82)	0.65 (1.12)	-0.16 (1.71)	-1.09 (2.57)	-0.50 (1.03)	<b>-1.17 (2.53)</b>
	mat-2	<b>0.74 (0.29)</b>	0.98 (0.37)	0.93 (0.22)	1.01 (0.28)	0.79 (0.25)	0.85 (0.22)
	mat-6	1.03 (0.25)	1.30 (0.06)	1.07 (0.19)	1.12 (0.20)	<b>0.98 (0.25)</b>	1.01 (0.23)
	mic-10	1.74 (0.11)	1.92 (0.07)	1.75 (0.09)	1.74 (0.10)	<b>1.70 (0.09)</b>	1.74 (0.11)
6	mic-5	<b>0.44 (0.32)</b>	0.96 (0.14)	0.55 (0.27)	0.63 (0.21)	0.50 (0.27)	0.63 (0.34)
	nrobot-4	-1.14 (0.88)	-1.24 (1.23)	<b>-1.73 (0.88)</b>	-1.48 (0.72)	-1.32 (0.83)	-1.24 (0.83)
	ack-10	-0.63 (0.27)	-0.01 (0.04)	<b>-0.65 (0.29)</b>	-0.37 (0.20)	-0.44 (0.25)	-0.43 (0.20)
	ack-5	<b>-1.19 (0.60)</b>	-0.39 (0.26)	-1.17 (0.65)	-0.39 (0.22)	-0.68 (0.41)	-0.87 (0.40)
	egg-2	-0.18 (1.05)	0.57 (1.15)	0.50 (0.94)	0.65 (0.98)	<b>-0.53 (1.40)</b>	-0.45 (0.99)
	mat-2	0.82 (0.25)	1.02 (0.20)	0.98 (0.34)	1.06 (0.23)	<b>0.81 (0.22)</b>	0.83 (0.24)
	mat-6	1.02 (0.24)	1.25 (0.16)	<b>0.99 (0.28)</b>	1.18 (0.27)	1.05 (0.23)	1.03 (0.23)
8	mic-10	1.77 (0.10)	1.92 (0.07)	<b>1.76 (0.08)</b>	1.76 (0.08)	1.76 (0.13)	1.77 (0.10)
	mic-5	<b>0.51 (0.34)</b>	0.96 (0.15)	0.66 (0.27)	0.72 (0.25)	0.66 (0.37)	0.63 (0.30)
	nrobot-4	-1.27 (0.80)	-1.12 (1.28)	-1.24 (0.89)	-1.03 (0.94)	<b>-1.35 (0.95)</b>	-1.27 (1.00)
	ack-10	-0.57 (0.22)	-0.01 (0.03)	-0.62 (0.26)	-0.44 (0.23)	-0.41 (0.25)	<b>-0.63 (0.16)</b>
	ack-5	-1.16 (0.47)	-0.42 (0.24)	<b>-1.32 (0.46)</b>	-0.47 (0.23)	-0.70 (0.51)	-1.12 (0.41)
	egg-2	-0.24 (0.91)	0.42 (1.13)	-0.02 (2.20)	0.78 (0.86)	-0.04 (0.54)	<b>-0.27 (0.85)</b>
	mat-2	0.78 (0.23)	0.90 (0.25)	0.81 (0.44)	1.09 (0.20)	0.81 (0.26)	<b>0.75 (0.30)</b>
16	mat-6	<b>1.01 (0.23)</b>	1.30 (0.09)	1.07 (0.17)	1.23 (0.17)	1.02 (0.19)	1.04 (0.25)
	mic-10	1.78 (0.08)	1.91 (0.07)	<b>1.72 (0.10)</b>	1.75 (0.09)	1.74 (0.13)	1.74 (0.08)
	mic-5	<b>0.46 (0.37)</b>	0.93 (0.19)	0.53 (0.35)	0.68 (0.26)	0.50 (0.32)	0.50 (0.52)
	nrobot-4	-1.24 (0.76)	-1.18 (1.23)	<b>-1.44 (0.84)</b>	-1.17 (0.98)	-1.35 (1.02)	-1.13 (0.85)
	ack-10	-0.44 (0.20)	-0.02 (0.04)	<b>-0.63 (0.24)</b>	-0.37 (0.18)	-0.40 (0.18)	-0.61 (0.16)
	ack-5	-0.83 (0.43)	-0.41 (0.23)	-1.03 (0.51)	-0.41 (0.24)	-0.43 (0.30)	<b>-1.11 (0.35)</b>
	egg-2	-0.41 (2.18)	0.34 (1.17)	0.83 (0.67)	1.21 (0.49)	<b>-0.86 (2.23)</b>	-0.53 (2.03)
	mat-2	<b>0.79 (0.26)</b>	0.88 (0.24)	1.07 (0.16)	1.12 (0.20)	0.86 (0.29)	0.83 (0.31)
	mat-6	1.09 (0.18)	1.31 (0.04)	1.02 (0.21)	1.21 (0.20)	<b>1.01 (0.23)</b>	1.02 (0.42)
	mic-10	1.80 (0.11)	1.90 (0.07)	1.75 (0.09)	1.77 (0.10)	1.76 (0.10)	<b>1.72 (0.13)</b>
	mic-5	<b>0.53 (0.33)</b>	0.91 (0.21)	0.68 (0.25)	0.67 (0.38)	0.66 (0.28)	0.60 (0.36)
	nrobot-4	-1.10 (0.86)	-1.15 (1.20)	<b>-1.39 (0.95)</b>	-0.95 (1.02)	-0.86 (0.60)	-1.07 (0.92)

Table 4. Mean and standard deviation of the log(regret) after 100 steps of asynchronous BO.

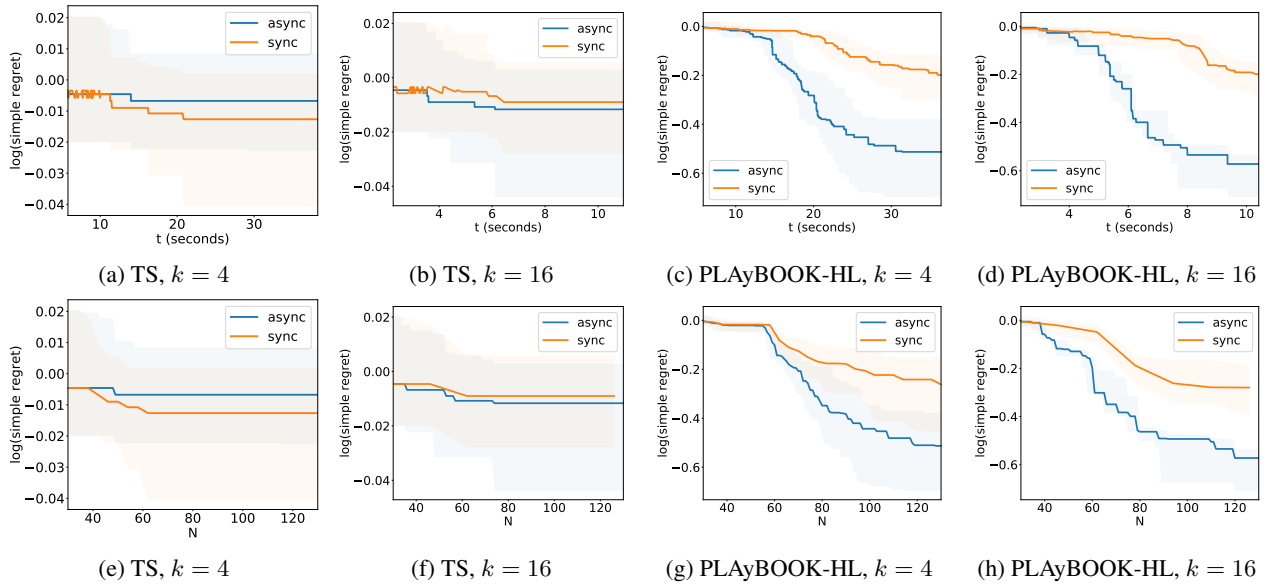


Figure 7. Head-to-head comparison on ack-10

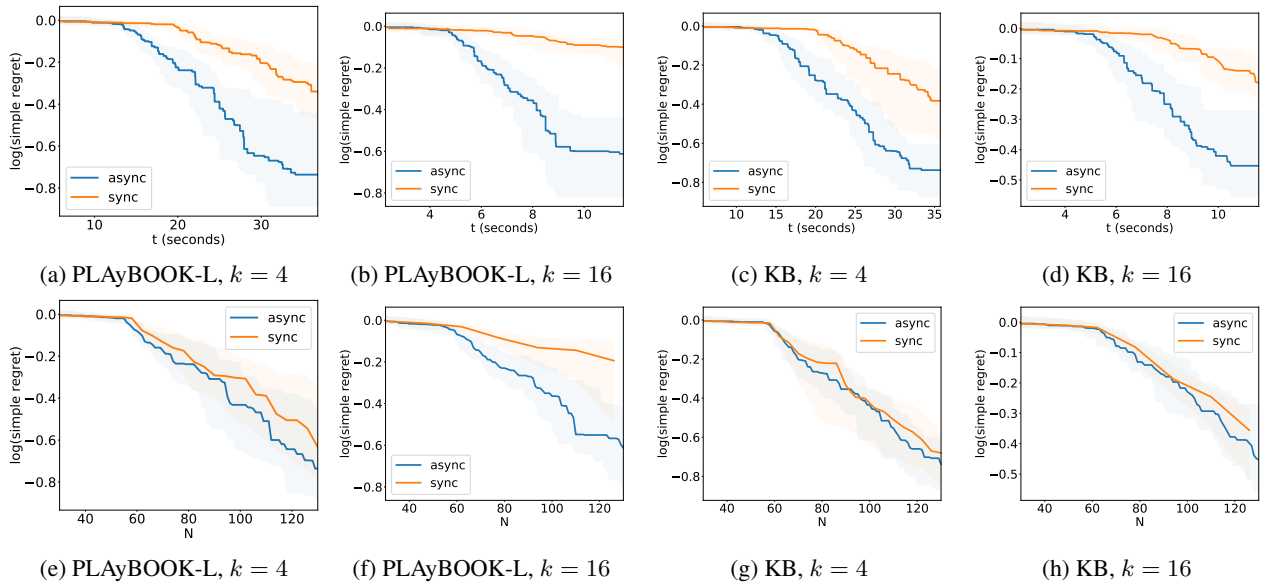


Figure 8. Head-to-head comparison on ack-10